A New Family of Soft Single Switched DC-DC Converters with Lossless Passive Snubber

Shabnam Nasr Esfahani[1], Majid Delshad[2*], Mohammad Bagher Tavakoli[1]
1- Department of Electrical Engineering, Arak Branch, Islamic Azad University, Arak, Iran.
Email:sh.nasr92@iau-arak.ac.ir, m-tavakoli@iau-arak.ac.ir
2- Department of Electrical Engineering, Isfahan (Khorasgan) Branch, Islamic Azad University, Isfahan, Iran.
Email: delshad@khuisf.ac.ir (Corresponding author)

Received: November 2019 Revised: March 2020 Accepted: April 2020

ABSTRACT:
In this paper, a novel lossless snubber is introduced that provides ZVS conditions for both On and Off instant of converter switches. On one hand, the energy of the snubber is optimally transmitted to the output so that no significant losses are imposed on the converter. Since the converter diodes are switched off as ZCS, the reverse recovery problem is reduced. In this paper, the proposed snubber circuit is applied to a conventional boost converter and an 80W sample is constructed in the laboratory to prove the performance and theoretical analysis. Furthermore, in order to confirm the effectiveness of the proposed snubber on the reduction of Electromagnetic Interference (EMI), the EMI value of the boost converter with the proposed snubber has been compared with the conventional boost converter, which shows a decrease of 10dBµV.

KEYWORDS: Lossless Passive Snapper, Zero Current Switching Condition (ZCS), Zero Voltage Switching Condition (ZVS), Electromagnetic Interference (EMI).

1. INTRODUCTION

DC-DC converters are widely employed in radio system [1], battery chargers equipment, telecommunications equipment [2], computers, fuel cells, televisions and many other industrial, telecommunication and high-tech military applications [3]. In order to reduce the weight and size of these converters, we have to increase their operating frequency, which increases the switching losses and creates electromagnetic interference [1-4]. On one hand, the use of the semiconductor switches for high power applications brings about issues such as the switching frequency limitation of the converters and increasing the stress of switching losses. One of the most common ways to provide soft switching conditions is the use of snubbers. Snubber circuits are designed to modify the shape of the switching waves, to reduce losses, and to have switch protection. Snubbers with RCDs and RLDs losses reduce the overall efficiency of the converter due to inducing losses to the converter. In snubbers without loss, the energy stored in the snubber's elements is either returned to the input or transferred to the output, and thereby increases efficiency. To eliminate switching losses, it is advisable to use snubbers that reduce both the instantaneous losses when switched on (current snubbers) and the instantaneous losses when switched off (voltage snubbers) [5].

These passive lossless snubber circuits are used because of their advantages in [6-15]. In [6], a passive lossless snubber circuit is used for non-isolated PWM converters, where the circuit switch is switched on under zero flow conditions and switched off under zero voltage conditions. Depending on the circuit composition, the amount of losses in the circuit can be reduced with the help of the snubber circuits and no power is dissipated in the passive components of this circuit. However, due to the presence of auxiliary inductor in the power converter path, the conductive losses are increased and the circuit performance is complicated. In [7], a family of single-switch converters with reduced stress is investigated in which all the semiconductor elements are soft-switched and switched on under ZCS conditions and switched off under ZVS conditions. There are coupled inductors in the circuit structure and the leakage inductance of these inductors cause unwanted resonance in the circuit. In [9], the reduction of switch-off losses was investigated with a passive lossless snubber switch for the boost converter. This snubber reduces switch-off losses in the boost mode. The applied snubber creates a path for the current at the moment of shutdown, and the switch turns off under ZVS conditions. The switch is also switched on under ZCS conditions and all other semiconductor elements are switched with soft switching conditions. However, this snubber is only applicable to the boost converter and cannot be applied to other circuits. In [10], a family of single switch converters is shown with a passive lossless snubber, which is added to a passive lossless snubber transducer, with all semiconductor elements being soft-switched. The circuit acts in such a way that energy, stored in the snubber circuit, is transmitted to the output, but the number of circuit elements is high and its operation is complex. In [11], an intermixed flyback converter with a passive lossless snubber is presented which has an inactive snubber. In the presented converter, the ripple current is reduced and the EMI is lower. The energy recycled in the snubber circuit is transferred to the output. All semiconductor elements of the circuit are soft-switched, but due to the high number of elements and coupled inductors in the circuit, it has a complicated operation. In [14], a high step-up converter with a new lossless snubber is presented where all semiconductor elements are soft-switched. There are coupled inductors in the circuit, the leakage inductance of these inductors causes unwanted resonance and increases conductive losses in the circuit. In [15], a passive lossless snubber cell is introduced to provide soft switching conditions for switches. All circuit diodes are soft-switched, and there are no reverse recovery problems in the diodes of the circuit. However, the main drawback of this design is the high voltage stress on the circuit switch and the presence of an auxiliary diode in the converter power path, which limits the use of these snubbers for high power converters.

2. THE INTRODUCED BOOST CONVERTER WITH THE LOSSLESS SNUBBER

The proposed snubber consists of two resonant capacitors C_1 and C_2, one resonant inductor (L_r), and three diodes (D_1-D_3) and two coupled inductors (L_1-L_2). The boost converter with the proposed snubber circuit is shown in Fig. 1.

To simplify the analysis of the converter and circuit, the following are considered during the analysis.

1- All elements of the circuit are considered ideal.

2. The inductors L_1 and L_2 are considered equal ($L_2 = L_1$).

3. The capacitors C_1 and C_2 are considered equal. ($C_2 = C_1$)

4. The value of the L_{in} inductor and C_O capacitor are considered large enough so they can be considered constant in a switching cycle with the current source (I_{in}) and voltage source (V_O), respectively.

The key shapes of the proposed converter are illustrated in Fig. 2. The following circuit has 7 operating statuses in a switch cycle. We will analyze the converter in each situation.

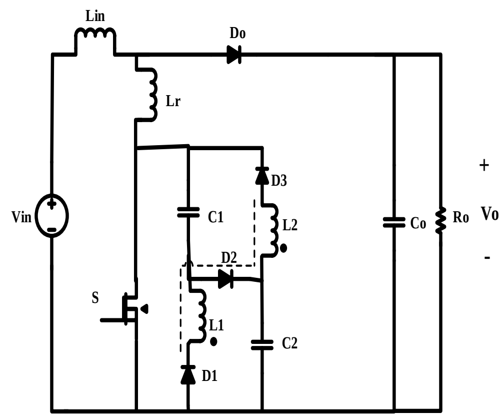

Fig. 1. The introduced boost converter with proposed snubber circuit.

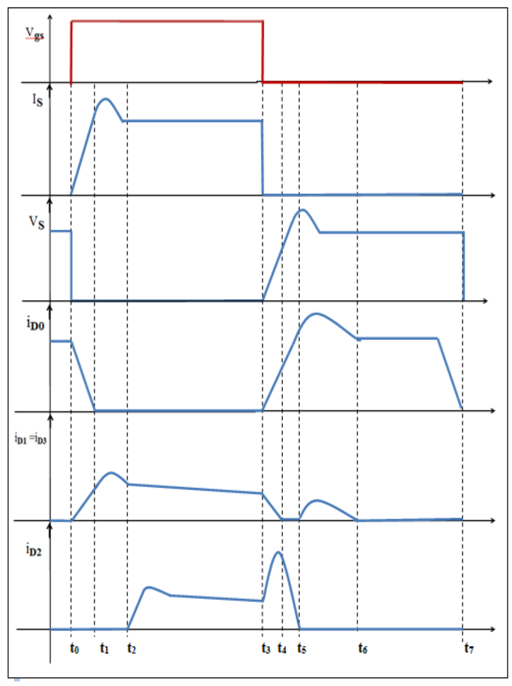

Fig. 2. Key waveforms of the proposed Boost converter with lossless snubber.

2.1. The Function of the Proposed Converter

The snubber inductors L_1 and L_2 provide ZCS soft switching conditions and prevent the di⁄dt increase when the S switch is switched on and also store all the transmitting energy of the snubber capacitors C_1 and C_2 when the S switch is switched off. In addition, the capacitors C_1 and C_2 guarantee the S switch to prevent dv⁄dt increase and create ZVS soft-switching conditions when it is switched off. The snubbers capacitors are charged up to $V_O/2$. Due to the Lr inductor, the snubber capacitors C_1 and C_2 must be discharged under ZVS conditions. When switch S is switched on, the snubber capacitors C_1 and C_2 transfer all their energy to the L_1 and L_2 inductors. Prior to the first mode, switch S and all the diodes of the circuit except for the D_O output diode are switched off and the energy of the L_{in} input inductor is transmitted to load.

- **Mode 1** [t_0, t_1]:

At the beginning of this interval, the main switch S is switched on ZCS conditions resonantly due to the increase in the current of L_1 and L_2 inductors and linearly due to the L_r inductor. In this mode, the switch current is the result of the sum of the currents of L_1, L_2 and L_r. The slow increase of these currents results in a slow decrease of the D_O diode output current. The end of this mode is when the output diode current D_O is zero. Important relationships are as follows:

$$i_{L_r}(t) = \frac{V_O}{L_r}(t - t_0) \tag{1}$$

$$i_{L1}(t) = i_{L2}(t) = \frac{V_O}{2Z_0} sin(\omega_0\,(t - t_0)) \tag{2}$$

$$V_{C1}(t) = V_{C2}(t) = \frac{V_O}{2}(1 - cos(\omega_0(t - t_0))) \tag{3}$$

$$Z_0 = \sqrt{\frac{2L}{C}} \tag{4}$$

$$\omega_0 = \frac{1}{\sqrt{2LC}} \tag{5}$$

$$i_S(t) = i_{Lr}(t) + i_{L1}(t) + i_{L2}(t) = \frac{V_O}{L_r}(t - t_0) + \frac{V_O}{Z_0} sin(\omega_0\,(t - t_0)) \tag{6}$$

The maximum S switch current equal to I_1 is when the angle value in equation (6) equals $\pi/2$. So this value is:

$$\omega_0(t - t_0) = \frac{\pi}{2}$$

$$I_1 = V_O\left(\frac{\pi\sqrt{2LC}}{2L_r} + \sqrt{\frac{C}{2L}}\right) + I_{in} \tag{7}$$

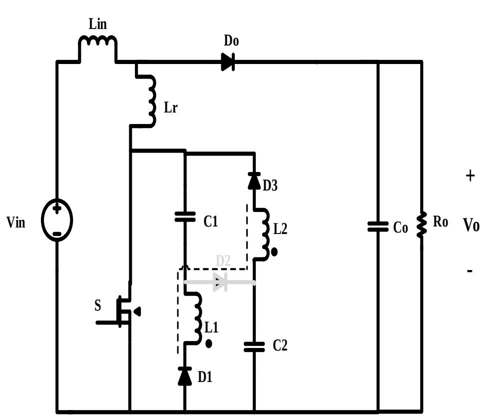

Fig. 3. The equivalent circuit operation of the proposed converter in the first Mode.

- **Mode 2** [t_1, t_2]:

At t_1, the output diode current D_O is zero and the output diode is switched off under ZCS conditions and this mode begins. According to equations (2) and (3), in this mode; the current of the L_1 and L_2 inductors, the voltage of the resonant capacitors C_1 and C_2 (which started between the inductor L_1 and capacitor C_1, and the inductor L_2 and capacitor C_2 in previous mode), and the resonant S switch current are increased. This mode ends when the voltage of the capacitors C_1 and C_2 are zero and the currents of the L_1 and L_2 inductors reach their maximum. Equations (2) and (3) remain true in this Mode.

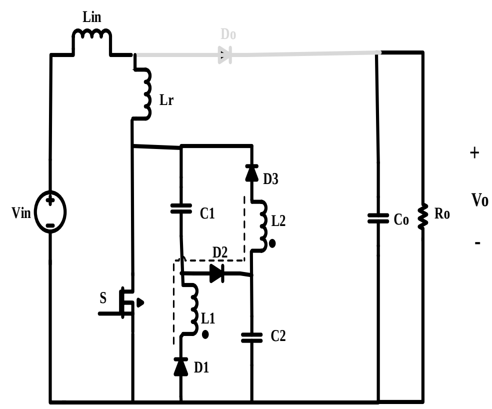

Fig. 4. The equivalent circuit operation of the proposed converter in the second Mode.

- **Mode 3** [t2, t3]:

This mode begins with the voltage of capacitors C_1 and C_2 reaching zero. Complete discharge of the capacitors and mounting them at the two ends of the D_2 diode will cause the diode to switch on under ZVS conditions. This results in the current of the L_1 and L_2 inductors, which were stored in the previous mode, to flow via the diodes D_1, D_2 and D_3 and switch S in freewheeling manner. In this case, the circuit is like a normal boost converter with the switch on, causing the input inductor(L_{in}) to start charging linearly. This mode ends with the S switch switching off.

$$i_{L_r}(t) = i_{L_{in}}(t) = i_{L_{in}}(t_2) + \frac{V_{in}}{L_{in}+L_r}(t - t_2) \tag{8}$$

$$i_S(t) = i_{L_r}(t - t_2) + \frac{V_0}{2Z_0} sin(\omega_0(t - t_2)) \tag{9}$$

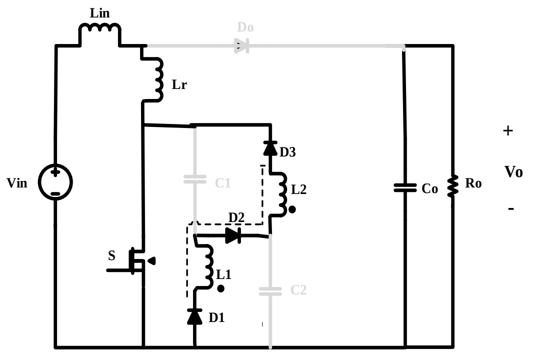

Fig. 5. The equivalent circuit operation of the proposed converter in the third Mode.

- **Mode 4** [t3, t4]:

This mode begins with the S switch switching off under ZVS conditions and the D_O output diode is switched on simultaneously under ZCS conditions. The capacitors C_1 and C_2, which were previously completely discharged, start to charge resonantly in this mode with the help of the currents in the L_1 and L_2 inductors. During this resonance, the voltage of the capacitors C_1 and C_2 increases and the currents of the resonators L_1 and L_2 decrease. Reduction of the inductors current causes the D_1 and D_3 diodes to switch off under ZCS conditions.

$$V_{C1}(t) = V_{C2}(t) = i_L(t_3) Z_1 \, sin(\omega_1 \, (t - t_3)) \tag{10}$$

$$Z_1 = \sqrt{\frac{L}{C}} \tag{11}$$

$$\omega_1 = \sqrt{\frac{1}{LC}} \tag{12}$$

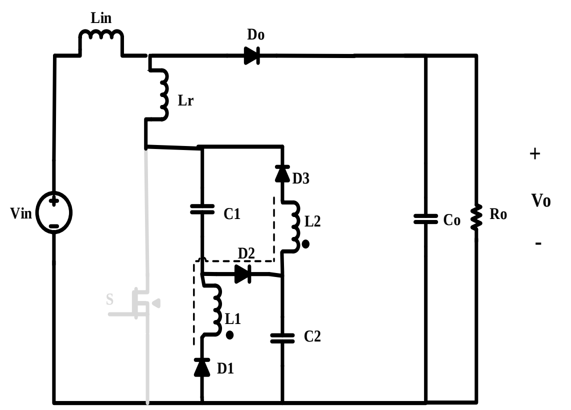

Fig. 6. The equivalent circuit operation of the proposed converter in the fourth Mode

- **Mode 5** [t4, t5]:

In this mode, the capacitors C_1 and C_2 start a new resonance with the L_r inductor and continue charging. This mode ends with the L_r inductor current reaching zero and D_2 diode switching off under ZCS conditions. The voltage equations for capacitors C_1 and C_2 are as follows.

$$V_{C1}(t) = V_{C2}(t) = V_C(t_4) + \, i_{L_r}(t_4) Z_2 \sin(\omega_2 \, (t - t_4)) \tag{13}$$

$$\omega_2 = \sqrt{\frac{2}{CL_r}} \tag{14}$$

$$Z_2 = \sqrt{\frac{2L_r}{C}} \tag{15}$$

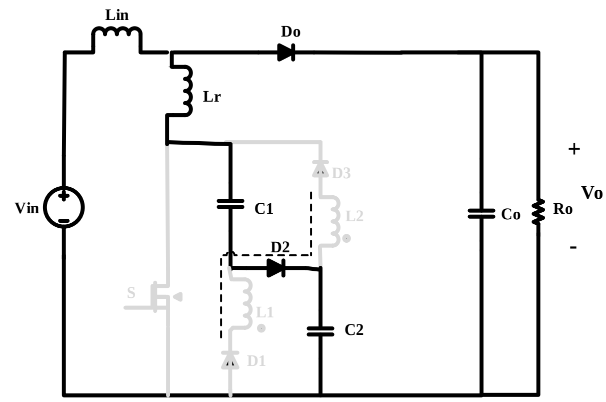

Fig. 7. The equivalent circuit operation of the proposed converter in the fifth Mode.

- **Mode 6** [t5, t6]:

At t5, capacitors C_1 and C_2 resonate with the L_1 and L_2 inductors, respectively, and transmit their energy to the output via the L_r inductor and D_O output diode. After half a resonance cycle, the currents of the L_1 and L_2 inductors become zero. The end of this mode is when diodes D_1 and D_3 are switched off under ZCS conditions.

$$V_{C1}(t) = V_{C2}(t) = V_C(t_5) + \, i_{L_r}(t_5) Z_1 \, sin(\omega_1 \, (t - t_5)) \tag{16}$$

$$i_{Lin}(t) = i_{Lin}(t_5) + \frac{V_{in} - V_O}{L_{in}} (t - t_5) \tag{17}$$

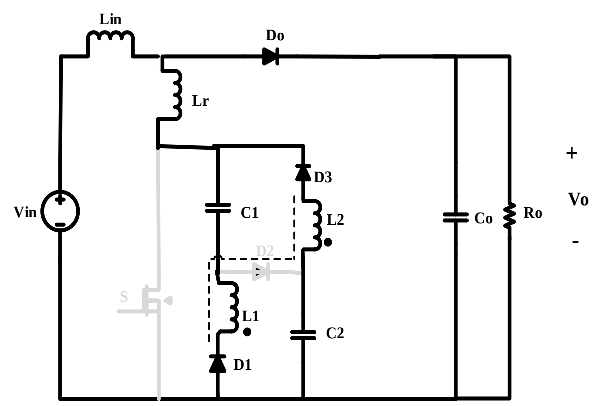

Fig. 8. The equivalent circuit operation of the proposed converter in the sixth Mode

- **Mode 7** [t6, t7]:

In this mode all the auxiliary diodes are switched off and the auxiliary circuit is completely disassembled according to Fig. 9. The function of the converter in this mode is similar to that of a normal boost converter with the switch off, and the energy stored in the L_{in} input inductors are discharged in the output.

$$i_{L_{in}}(t)=i_{L_{in}}(t_6)+\frac{V_{in}-V_O}{L_{in}}(t-t_6) \quad (18)$$

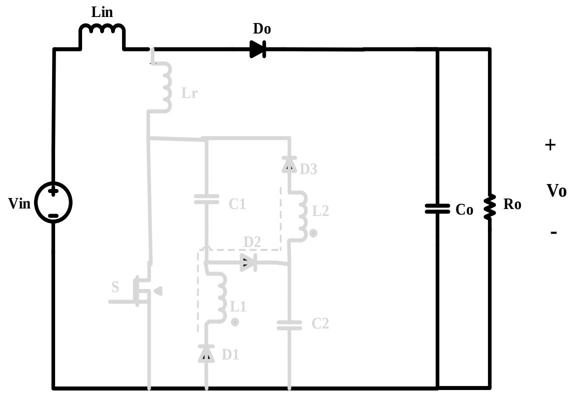

Fig. 9. The equivalent circuit operation of the proposed converter in the seventh Mode.

3. DESIGN OF THE PARAMETERS FOR THE PROPOSED CONVERTER

Since the design of the proposed converter is similar to that of conventional boosts, this section deals with the design of the elements used in the proposed lossless snubber. In the first step of the design, the value of the snubber capacitor should be calculated. In order to create ZVS conditions for switch S, capacitor C can be designed using the following relation: [16]

$$C_1 = C_2 = \frac{i_{Lin}.t_f}{2V_{SW}} \quad (19)$$

i_{Lin}: The current flowing in L_{in} before the switch switching off.
tf: The switch converter voltage drop time.
V_{SW}: The final voltage of the switch after switching off.
To create ZCS conditions for the converter switch when it is switched on, L_r is obtained from the following equation: [16]

$$L_r = \frac{V_{SW}.t_r}{I_{SW}} = \frac{V_O.t_r}{I_{in}} \quad (20)$$

t_r: Current increase time,
I_{SW}: the final current of converter switch after switching it on and V_{SW}: the final voltage of the circuit switch before switching the switch off.

During the time that the switch is on, the snubber capacitors should be completely empty, so the resonance start time is important in the first mode.

As mentioned in the previous section, after half a resonance cycle between the capacitors C_1 and C_2 and the inductors L_1 and L_2, the voltage of the snubber capacitors becomes zero, so this time should be less than the minimum switch on time ($D_{min}T_{sw}$), and so we have:

$$C_1=C_2=C$$
$$L_{1,2} < \frac{D^2(min)}{2\pi^2.C.f_{SW}{}^2} \quad (21)$$

D(min): Minimum duty cycle

4. EXPERIMENTAL RESULTS OE THE PROPOSED CONVERTER

In this section, a prototype of the Boost Converter was made to confirm the accuracy of the analysis for the proposed converter. The values and specifications of the proposed converter elements are given in Table 1. The image of the implemented circuit is shown in Fig. 10. The measured waveforms of the current and the voltage of the switch and the diode current confirm the theoretical analysis.

Table 1. The parameters of the introduced converter.

Elements	Value
L_{in}	400μH
L_r	5μH
$L_1=L_2$	10μH
$C_1=C_2$	10nF
C_O	47μF
All Diodes	MUR 860
Switch	IRF 640
f_{SW}	100KHz
V_{in}	24V
V_{out}	48V
P_{out}	80W

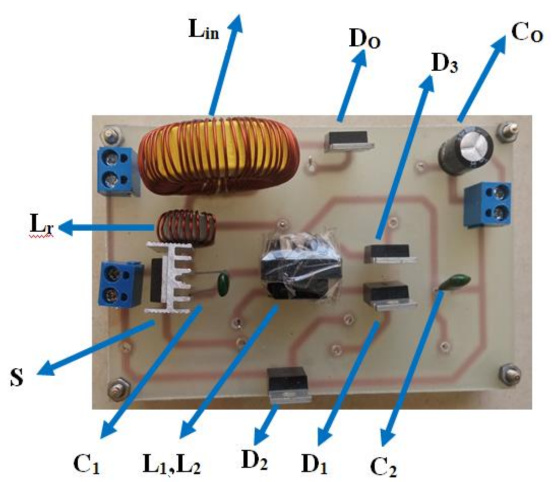

Fig. 10. Proposed Boost Converter Circuit.

Fig. 11 shows the voltage and current waveforms of the switch. It can be seen in the figure that the switch is switched on under ZCS conditions and switched off under ZVS conditions. As can be seen, the switch voltage has a certain overshoot due to the resonance between the parasitic switch capacitor and the L_r inductor.

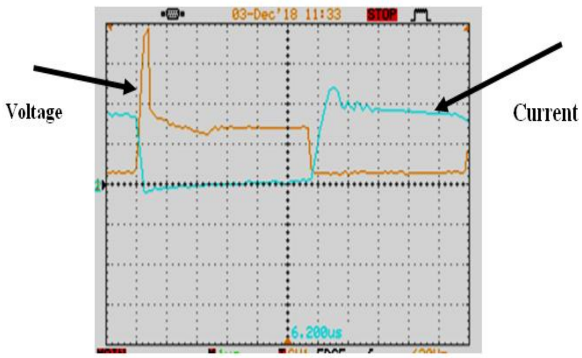

Fig. 11. The voltage and current waveforms of the switch (50V / div, 2A / div, 1µ s / div).

The switch current stress is controllable by changing the impedance of the resonance tank; according to equation (9) the switch current stress decreases with increasing Z0. However, the amount of leakage inductance in the circuit increases the induction of the circuit coupling and causes an undesired rotation in the switch and diode circuit snubbers, which increases the value of the L_2, L_1 inductor snubbers.

The flow patterns of diodes D_1, D_2 and D_3 are shown in Figs. 12 and 14, respectively.

As shown in this figure, the diode flow has increased and decreased with a slope. As can be seen from these figures, diodes D_1, D_2 and D_3 are switched on and off by soft switching. This reduces reverse recovery losses in diodes. Fig. 15 shows the diode current output of the D_O circuit.

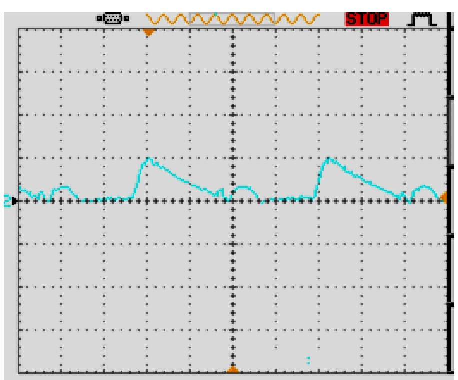

Fig. 12. Current waveform of D_1 in the proposed boost converter (1A / div), time (2.5µs / div).

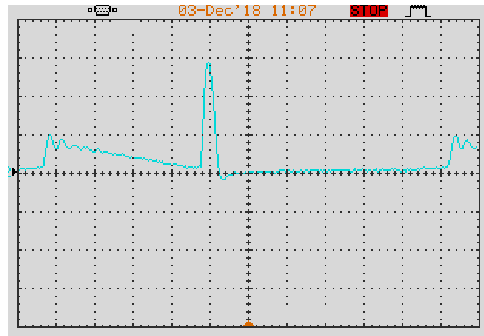

Fig. 13. Current waveform of D_2 in proposed boost converter (1A / div), time (1µs / div).

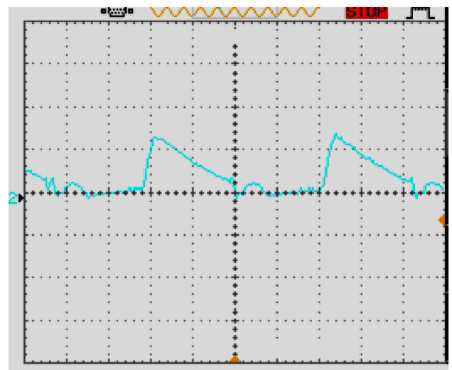

Fig. 14. Current waveform of D_3 in the proposed boost converter (1 A / div), time (2.5µs / div).

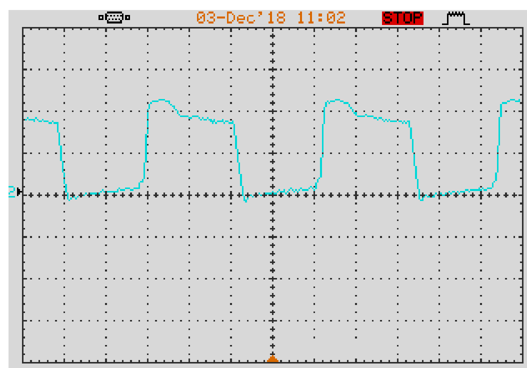

Fig. 15. Current waveform of D_O in the Proposed Boost Converter (2 A / div), Time (2.5µs / div).

As can be seen in Fig. 16, the D_O output diode is turned on and off by ZCS due to the presence of the L_r inductor. Therefore, not only are there no switching loss in the output diode but its reverse recovery problem is also solved.

5. INTRODUCTION TO OTHER SOFT SWITCHING CONVERTERS BY THE PROPOSED LOSSLESS SNUBBER CIRCUIT

The proposed snubber circuit has the capability to be applied to isolated base converters including Buck, Cuk, Buck-Boost and Sepic converters. The performance of these converters is similar to the one proposed in the previous section. The proposed snubber circuit can easily accommodate the transformer leakage inductors of the isolated converters and this is one of the advantages of the introduced snubber circuit. These converters are shown in Fig. 16.

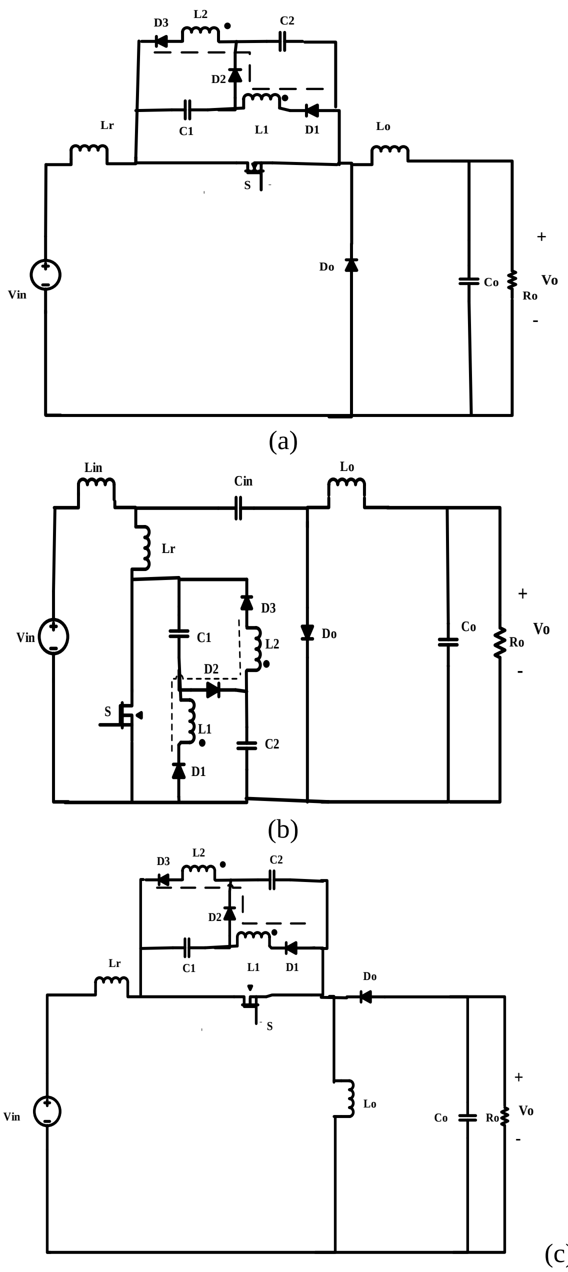

(a)

(b)

(c)

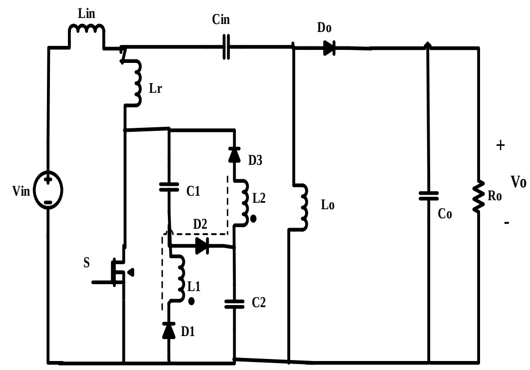

(d)

Fig. 16. Other proposed soft switching converters with the lossless snubber circuit (a) Buck, (b) Cuk , (c) Buck-Boost, (d) Sepic.

6. THE MEASURED EMI CONDUCTIVITY OF THE PROPOSED CONVERTER

In this section, a LISN CISPR22 is inserted at the entrance of the proposed transducer to measure the conductive Electromagnetic Interference (EMI) [17-18]. The Gw-Instek GSP380 spectrum analyzer in Fig. 17 was used to display the generated EMI value and was placed at the two ends of the RS resistor. The bandwidth resolution is set to 30kHz and electromagnetic interference is measured according to the CISPR22 standard from 150kHz to 30MHz.

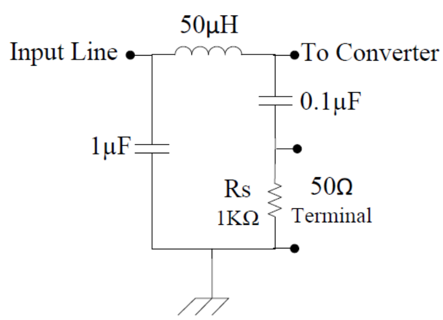

Fig. 17. CISPR22 LISN Model for Measurement of Conductive Electromagnetic Interactions [17].

The impact of the proposed snubber circuits for reducing the conductive EMI value is shown in Fig. 18. The figures shown illustrate that the peak conductive EMI for the proposed converter is about 89dBμV, which, in comparison to its hard switching counterpart, has reduced the EMI peak by approximately 10dBμV, indicating better performance of the proposed converter.

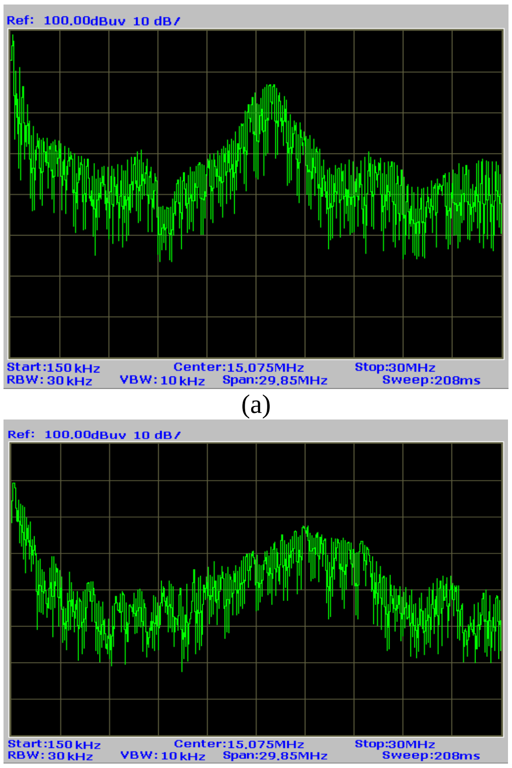

(a)

(b)

Fig. 18. Measured EMI Conductivity (a) Hard Switching Boost Converter, (b) Proposed Boost Converter (Vertical axis: 20–100 dBμV, horizontal axis: 0.15–30 MHz).

7. THE EFFICIENCY OF THE PROPOSED CONVERTER

In order to obtain the efficiency of the proposed converter, it is necessary to calculate the losses of the proposed converter elements.

The ohmic losses of the inductor in the circuit can be calculated from the following equation:

$$P_{loss,R_x} = \frac{1}{T}\int R_x . i_x^2 . dt \tag{22}$$

Where, Rx is the ohmic value of the inductor coils in the circuit. In addition, the core losses of these coils, which include Foco and Hysteresis losses are derived from the technical specifications of the inductor core (a relation between the switching frequency and the magnetic flux density). It should be noted that because the L_{in}-inductor current is in the continuous-flow mode, its core losses are negligible and its ohmic losses can be calculated from equation (22).

Switching losses of the switch converter can be calculated from the following equations.

$$P_{loss,S,ON} = \frac{1}{2} V_S I_S t_r f_{sw} \tag{23}$$

$$P_{loss,S,OFF} = \frac{1}{2} V_S I_S t_f f_{sw} \tag{24}$$

Since the circuit switch turns on and off softly, the switching losses of the converter switch are negligible in the soft mode and also the conductive losses of the converter switch can be calculated from the following equation.

$$P_{loss,S} = \frac{1}{T}\int R_{DS(ON)} . i_S^2 . dt \tag{25}$$

Switching diodes losses in the converter include the instantaneous switch-on losses of the converters and the instantaneous switch-off losses of the converters' diodes, which can be calculated from the following equations.

$$P_{loss,D,ON} = \frac{1}{2} V_D I_D t_{rr} f_{sw} \tag{26}$$

$$P_{loss,D,ON} = P_{loss,D,OFF} \tag{27}$$

Since the converter diodes are switched on and off softly, the switching losses of these diodes are negligible in the soft mode and the conductive losses of the converter diodes can be calculated from the following equation.

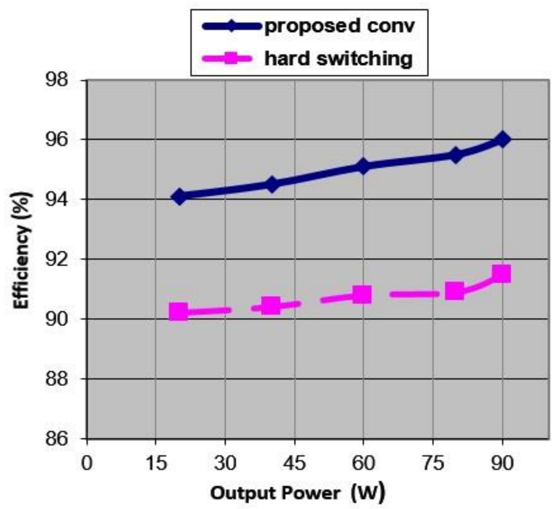

Fig. 19. The proposed Boost Converter efficiency compared to its hard switching counterpart.

$$P_{loss,D} = \frac{1}{T}\int V_F . i_D . dt \tag{28}$$

Hard switching boost converter losses include L_{in} inductor losses, S switch losses, and D_O diode losses, which are negligible due to the continuity of the Lin Inductor current, and only considered ohmic losses, which can be calculated from equation (22). In the case of the losses in switch S, the switching losses of the switch-on and switch-off moment can be calculated from equations (23) and (24) and the switch conductive losses from (25). In the case of D_O diode losses, the switching losses of the diode switch-on and the diode switch-off moment can be calculated from the equations (26) and (27) and the conductive losses of the D_O output diode from equation (28).

According to the above, the efficiency of the proposed converter has been measured at 5 different loads, and as shown in Fig. 19, the proposed full load boost converter yield has increased by 5% compared to the normal boost converter. There was less increase in efficiency when a lower load was applied.

8. CONCLUSIONS

The lossless passive snubber cell proposed in this paper provides the ZCS switch-on and the ZVS switch-off conditions for the circuit. The proposed snubber can be used for all basic DC-DC converters. All diodes in the proposed snubber are switched on and off under ZCS conditions, so there are no inverse recovery diode problems in the circuit. The proposed snubber is applied to the boost converter and is fully analyzed. Experimental results of the proposed converter show a 5% increase in nominal load efficiency compared to the conventional boost converter. In addition, in the proposed converter the electromagnetic interference decreased by 10dBμV compared to the hard switching counterpart.

REFERENCES

[1] T.Mishima, M.Nakaoka,**"A New Family of Soft Switching PWM Non-isolated DC-DC Converters with Active auxiliary Edge-Resonant Cell",** *IEEE Conferences, Power Electronics Conference (IPEC*), pp. 2804 – 2809, 2010.

[2] A.K.Panda, S.Pattnaik and K. K. Mohapatra, **"A Novel Soft-Switching Synchronous Buck Converter for Portable Applications",** *International Journal of Power Management Electronics, Article ID 862510*, 2007.

[3] S. -Y. Tseng, Y. –J. Li and, Y. –J. Wu, **"Buck Converter Associated with Active Clamp Flyback Converter for PV Power System**", *Green Power Evolution Applied Research Lab (G-PEARL), ICSET* 2008.

[4] E.Adib and H. Farzanehfard, **"New Zero Current Transition PWM Converters**", *in Proc. IEEE ICIT Conf.*, pp. 2131–2136, 2006.

[5] D.W. Hart, **" Power Electronics"**, *McGraw-Hill Companies Inc, New York*, 4th edn ,2010.

[6] C.-J. Tseng and C.-L. Chen, **"A Passive Lossless Snubber Cell for Nonisolated PWM DC/DC Converters"**, *IEEE Transactions on Industrial Electronics*, Vol.45 No.4, pp. 593-601, 1998.

[7] M.KHalilian,E.Adib andH.Farzanehfard**,"Familiy of Single-switch Soft-switching Pulse-width Modulation DC-DC Converters with Reduced Switch Stress"** , *IET Power Electronics*,Vol. 7, Iss. 8, pp. 2182–2189, 2014.

[8] M.Mohammadi, E.Adib and H.Farzanehfard,**" Passive Lossless Snubber for Double-Ended Flyback Converter"**, *IET Power Electronics*, Vol. 8, pp. 56 – 62, 2014.

[9] M.Mohammadi, E. Adib,**"Reducing Turn Off Losses with a Passive Lossless Snubber for Boost Converter"**, *Proc. 5th PEDSTC, Tehran, Iran*, pp. 385–389, 2014.

[10] M.Mohammadi, E.Adib and M. R. Yazdani, **"Family of Soft-Switching Single- Switch PWM Converters with Lossless Passive Snubber"**, *IEEE Transactions on Industrial Electronics,* Vol. 62, No. 6, pp. 3473-3481, 2015**.**

[11] N.Mohammadian, M.R.Yazdani**," Half-bridge Flyback Converter with Lossless Passive Snubber and Interleaved Technique"**, *IET Power Electronics*, Vol. 11, pp.239-245, 2017.

[12] J.W.Kim, J.M.Choe and J.Sh.Jason Lai, **"Nonisolated Single-Switch Two-Channel LED Driver with Simple Lossless Snubber and Low-Voltage Stress"**, *IEEE Transactions on Power Electronics*, Vol. 33, pp. 4306 – 4316, 2017.

[13] K.Soltanzadeh, M.R.Yousefi**,"Analysis and Design of Two-switch Flyback Converter with Double Passive Lossless Snubber"**, *IET Power Electronics(IET Journals & Magazines)*, Vol. 11, pp.1187 – 1194, 2018.

[14] S.W.Lee, H.L.Do**," High Step-Up Coupled-Inductor Cascade Boost DC–DC Converter With Lossless Passive Snubber"**, *IEEE Transactions on Industrial Electronics(IEEE Journals & Magazines)*, Vol. 65, pp.7753 – 7761, 2018.

[15] E.Gerami, M.Delshad, M.R.Amini and M.R.Yazdani**," A New Family of Non-isolated PWM DC–DC Converter with Soft Switching "**, *IET Power Electronics(IET Journals & Magazines)*, Vol. 12, pp. 237 – 244, 2018.

[16] T. M. U. W. P. R. Ned Mohan, **"Power Electronics: Converters, Applications, and Design**", *Michigan: John Wiley & Sons*, 2003.

[17] C.R. Paul, **"Introduction to Electromagnetic Compatibility"**, *publisher: J.Wiley and Sons, 2th Edition*, 2006.

[18] S. Wang, **"Characterization and Cancellation of High-Frequency Parasitic for EMI Filters and Noise Separators in Power Electronics Applications"**, *Ph.D Thesis, Virginia Tech*, May 2005.